J. Sci. Kharazmi University Vol. 13, No. 2

Summer 2013

Investigation of AC and DC Electrical Properties and Surface Morphology of Al/TiO2/PSi/Al Nanostructure

M. E. Azim Araghi, E. Khalili Dermani*;
Department of Physics, Kharazmi University

Abstract

In this research work nano porous silicon layers with different porosity were prepared by using electrochemical etching. Surface morphology and size of pores were investigated by scanning electron microscopy (SEM).TiO_2 thin films with EBPVD method have been deposited on the surface of PSi layers. The influence of anodization conditions such as anodization time interval and current density on electrical properties and surface morphology of sandwich devices were carried out using I-V measurements .The results showed that, electrical properties were influenced by changes of current density and anodization time interval. We also investigated the AC electrical conductivity of Al/TiO_2/PSi/Al sandwich devices over the range of frequency 10^2 to 10^5 Hz and temperature range 300 to 378 K. It is known that, over the range of frequency < 10^3Hz the band theory and over the range of frequency > 10^3Hz hopping mechanism is applicable in explaining the conductivity of TiO_2/PSi thin films nano structures with aluminum electrodes.

Introduction

At present PSi (Porous Silicon) has been extensively applied in various fields such as dielectric materials, gas sensors and optoelectronic application due to luminescence properties at room temperature and large surface area [1-3]. PSi layers consist of a network of nanometer – sized silicon regions surrounded by void space. The PSi matrix is characterized by the dimensions of the pores, ranging from the micro porous

Keywords: Thin films, Sandwich devices, Electrical conductivity.

Received: 19 Dec 2012 Revised 18 Dec 2013

*Corresponding author: ensieh_khalili@yahoo.com

[Downloaded from ndea10.khu.ac.ir on 2026-11-02]

(d_{pore}<2nm), meso porous (2nm<d_{pore}<50nm) and macro porous (d_{pore}>50nm) [4]. The most common method for fabrication PSi is electrochemical etching in HF-based solutions [5]. The variation of electrochemical conditions (current density, anodization time, composition of electrolyte) allow to change the silicon crystalline sizes in the wide range and vary the thickness of layers from 100 nm to 100μm [1]. In recent years, many efforts have been devoted to the preparation of sandwich devices, which consist of PSi and nano materials which can improve electrical and optical properties of PSi such as CdS, ZnO and ZnS [6]. The surface morphology and the electrical properties of PSi prepared from the single crystal silicon coated with a metal oxide film were showed obvious differences from that of the normal PSi. In order to modify the electrical properties of PSi for electronic and optoelectronic application, we can use the metal oxide thin film such as TiO_2 on the surface of PSi [7]. For its wide band gap, high refractive index and chemical stability [8], poly crystalline TiO_2 films are used for a variety of applications such as dye-sensitized solar cells [9], dielectric application [10], self-cleaning purposes [11] and photo catalytic layers [12]. Nano crystalline TiO_2 films consist of small particles with diameters less than 1μm, which are densely packed and form a highly porous structure [13]. A large number of investigations have been carried out on electrical and optical properties of porous silicon and TiO_2 thin film [14-15], but relatively little work has been done on the properties of porous silicon coated with TiO_2 thin film [16]. In this research work we prepared PSi samples with electrochemical etching and TiO_2 thin films have been deposited with EBPVD (Electron beam physical vapor deposition) method on the surface of PSi layers. The effect of anodization condition on morphology and electrical properties of samples has been investigated. Finally we describe the DC and AC electrical properties of Al/TiO_2/PSi/Al nano structures at different room temperatures.

Experimental Method

Monocrystal silicon substrates of p-type, B-doped, (100) orientation, resistivity of 0.05 Ω-cm and thickness of about 525μm were cut in to 1cm^2 square plates. An ohmic

[Downloaded from ndea10.khu.ac.ir on 2026-11-02]

contact was obtained by evaporating a thin Al film on the back side of the wafer. Before anodization, the samples were immersed in the HF aqueous solution to remove native oxide from the silicon surface, and washed with RCA (Radio Corporation America) method. The PSi layer was obtained by anodization in a (1:3:1) HF (%38):C_2H_5OH (%98):H_2O solution. Anodization was carried out with a platinum cathode. The current density and anodization time were varied from 15-35 (mA/cm^2) and 20-40 minutes respectively. The porosity of PSi layers was found using gravimetric method [17]. The samples were then immersed in ethanol, dried in the air, and placed in the electron-beam evaporation chamber for deposition of the TiO_2 layers. The TiO_2 metal oxide tablet-target was deposited with thickness of about 43 nm by using electron-beam evaporation. After the deposition process was completed, the thin films were annealed at 500 °C for 20 minutes. The TiO_2 thin films were coated with aluminum electrode as the metal contact. Metal contact was deposited by using thermal evaporation method. Finally, the samples were characterized. The crystalline properties of the TiO_2 thin films were obtained by an X-ray diffract meter (Equinox 3000) with wavelength of Cukα1 radiation. The morphology of all the PSi layers and TiO_2 thin film were recorded with a PhilipsXL30 scanning electron microscope (SEM). For DC electrical properties I-V measurements have been obtained by using a Kithley 610C electrometer. Finally the AC electrical conductivity was investigated by using MT 4080 LCRmeter in different room temperatures.

Results and Discussion

1. Surface morphology

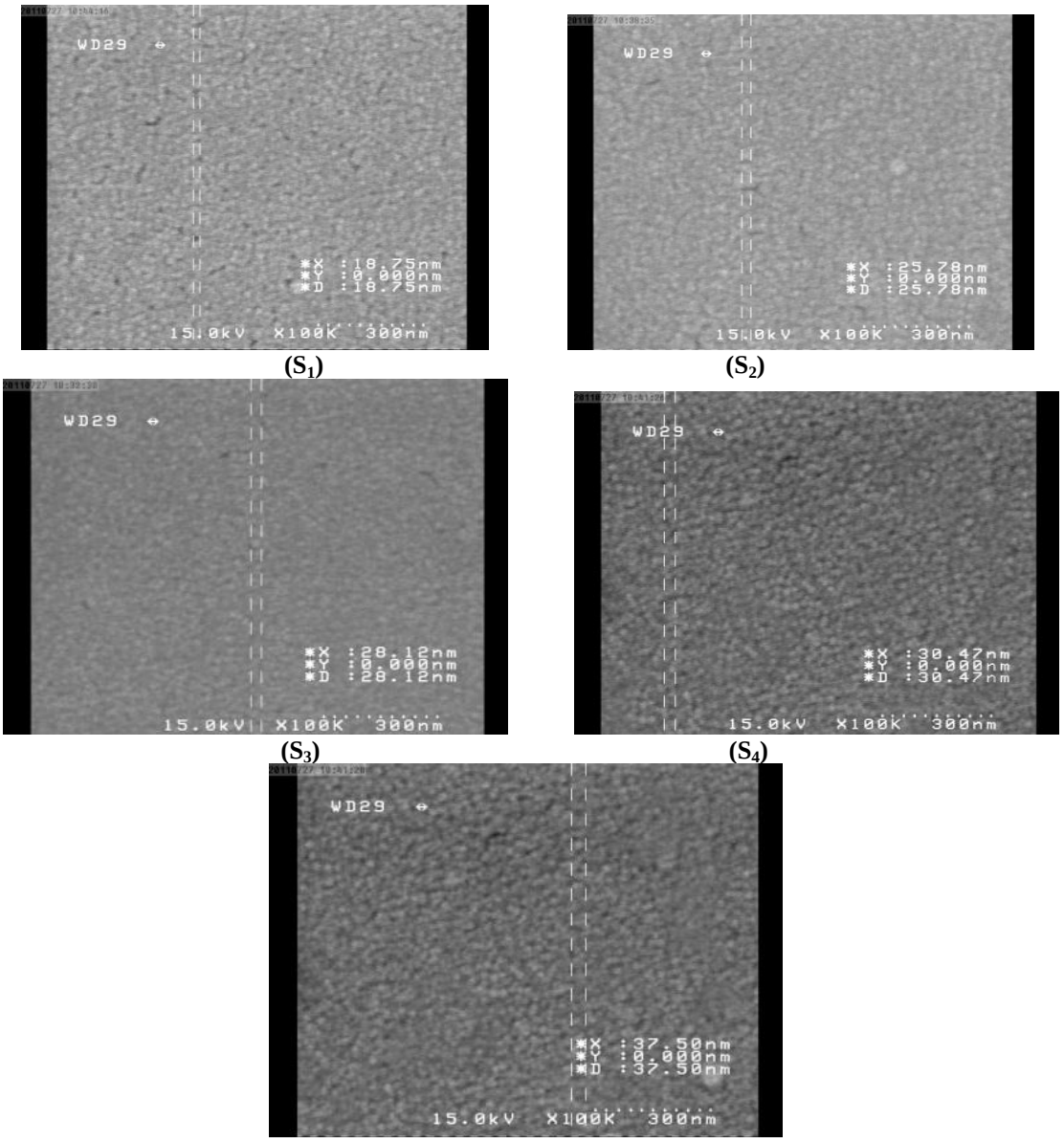
The variation of porosity in samples prepared with various anodization time intervals and the current density is presented in Table 1. We can see that, the porosity of PSi depends on anodization time and current density. The porosity increases with increasing current density and anodization time. The porosity of samples was calculated via the following formula [17]:

[Downloaded from ndea10.khu.ac.ir on 2026-11-02]

$$P = \frac{m_1 - m_2}{m_1 - m_3} \quad (1)$$

Where m_1 and m_2 are the masses of the samples before and after anodization, respectively, and m_3 is the mass after dissolution of the porous layers in NaOH solution.

Fig. 1 shows the morphology and pore size of samples with various anodization time intervals and current density. The electron micrograph of samples reveals that for samples with lower current density and anodization time, the pore diameters are smaller than the samples with higher current density and anodization time.



(S_1) **(S_2)** **(S_3)** **(S_4)** **(S_5)**

Fig. 1. SEM images from samples with a different anodization time and current density

[Downloaded from ndea10.khu.ac.ir on 2026-11-02]

Fig. 2 illustrates the XRD pattern of TiO_2 thin films which was deposited at room temperature and annealed at 500 ℃ for 20 minutes. It was found the film to be poly crystalline having anatase phase with lattice parameter a=0. 3785 nm matching well that of the reference data. The (101) lattice plane diffraction peak is observed to have the highest intensity

Table1. Dependence of porosity on anodization time and current density

	Current density (mA/cm^2)	Anodization time (minutes)	Porosity (%)
S1	15	20	40
S2	15	30	49
S3	15	40	56
S4	25	20	61
S5	35	20	69

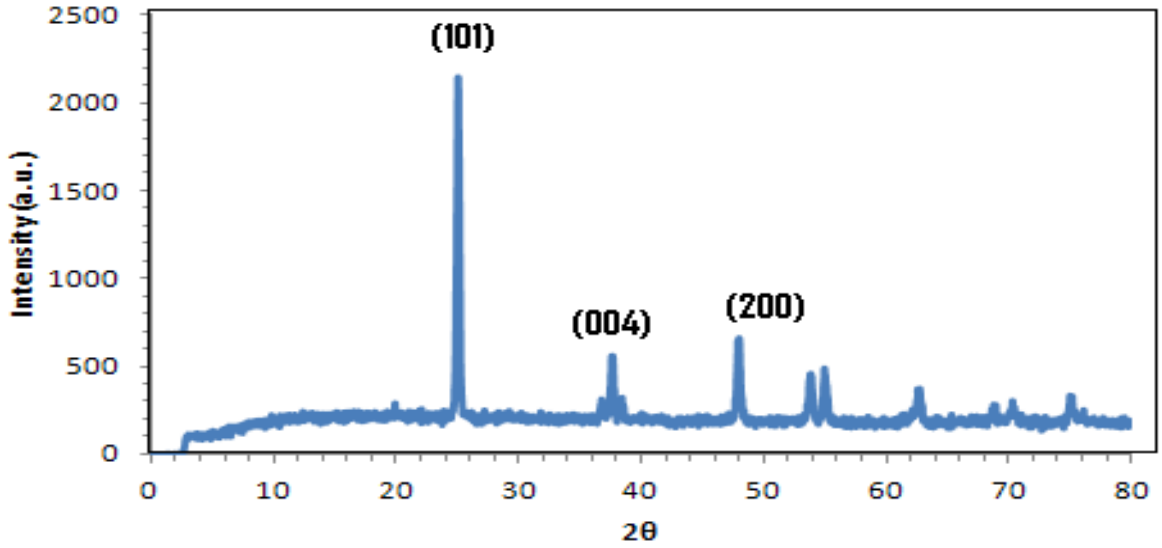


Fig. 2. XRD pattern of TiO2 thin film

The surface morphology of TiO_2 thin films is presented by SEM method. The SEM image (Fig. 3) Shows that the presence of TiO_2 nano particles combined together and formed a thin film. The average grain size of nano particles is about 73 nm.

3-2 DC electrical properties

The DC electrical properties of Al/TiO_2/PSi/Al sandwich devices were analyzed by performing I-V measurement of the thin films. All measurements were taken in dark conditions. A strong non-linear effect showed in fig. 4. From the graph, it showed that the samples exhibit a rectifying junction response with applied voltage. With deposition

[Downloaded from ndea10.khu.ac.ir on 2026-11-02]

TiO_2 on the surface of PSi we have a p-type/n-type semiconductor contact between TiO_2 and PSi. With applied forward voltage, forward current increased exponentially by applying a voltage. Increasing current density or anodization time interval increases the current for all forward biases, due to increasing the porosity of layers and increased the large surface area

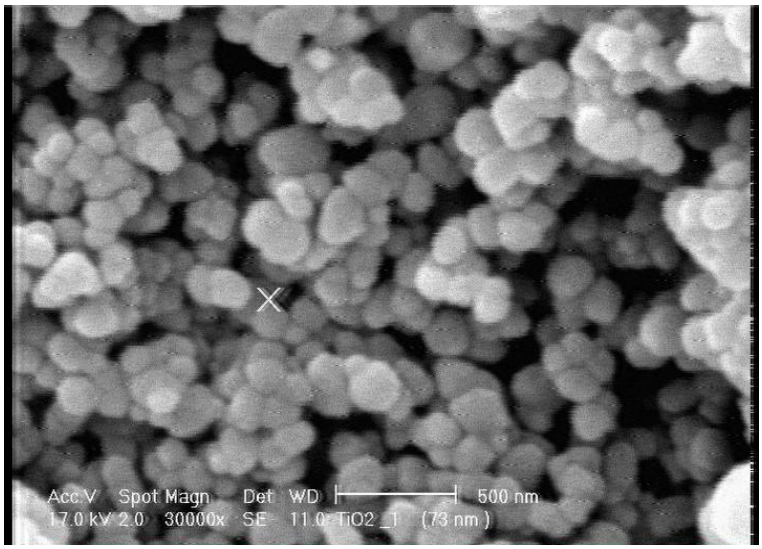


Fig. 3. SEM image of TiO2 thin film (the average grain size is 73 nm)

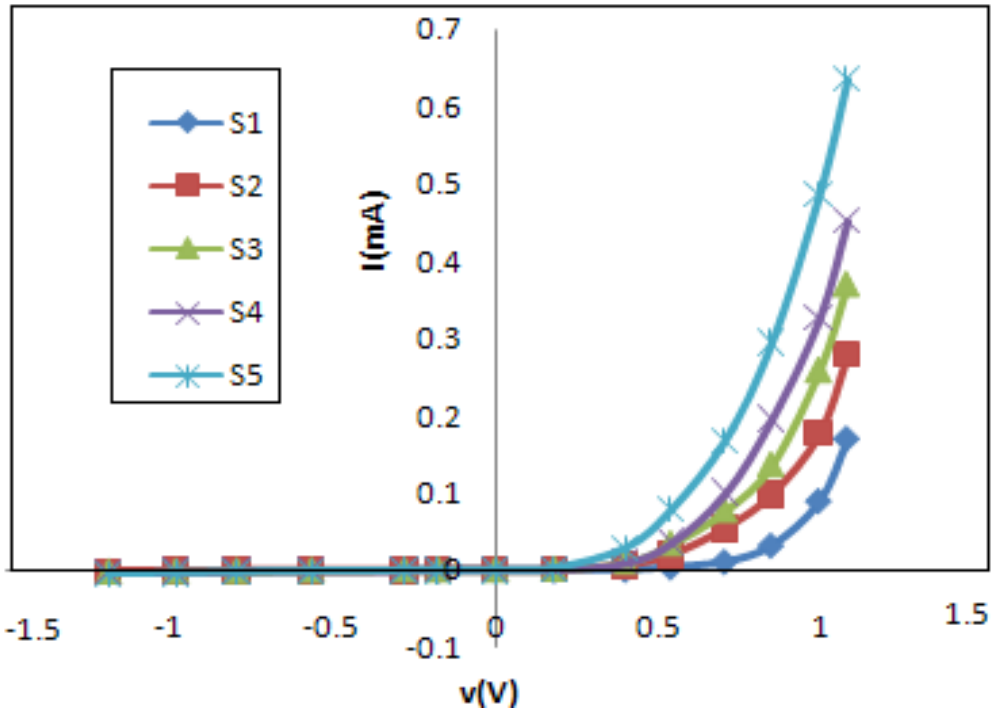


Fig. 4. I-V characteristic curves of Al/TiO_2/PSi/Al structures with different porosity

[Downloaded from ndea10.khu.ac.ir on 2026-11-02]

3-3 AC Conductivity

The AC electrical conductivity was calculated from the below equation:

$$\sigma_{AC} = \omega c \tan\sigma \quad (2)$$

Where ω is the angular frequency, c is the capacitance and tanσ is the dissipation factor.

The measurement performed for the sample was made with 35 (mA/cm^2) current density and 20 minutes anodization time. The results are shown in Fig. 5. The conductivity data exhibit strong frequency dependence. It was found that at low frequencies the conductivity decreases with increasing frequency at constant temperature, but in high frequencies the conductivity increases with increasing frequency. The conductivity is a decreasing function of frequency in the case of band conduction and an increasing function of frequency in the case of conductivity by hopping mechanism. Over the range of frequency < 10^3 Hz the band theory is applicable to explain the conduction process in $Al/TiO_2/PSi/Al$ nano structures and in the range of frequency >10^3, the increasing of slope with increasing frequency connected with hopping conduction mechanism [18].

The conductivity of a semiconductor material can be expressed as [19]:

$$\sigma = \sigma_{DC} + \sigma_{AC} \quad (3)$$

The first part is the DC conductivity which is due to band conduction. The second part of this relation is pure AC conductivity which is due to correlated barrier hopping (CBH) process. In general the AC conductivity has a frequency dependence given by

$$\sigma_{AC} = A\omega^S \quad (4)$$

Where A and S are characteristic parameters which depend both on temperature. The temperature dependence of the index S can be expressed as [20]:

$$S = 1\text{-}6\ K\ T/W_M \quad (5)$$

Where W_M is the maximum barrier height. A decrease of W_M upon the temperature increase was observed. It can be seen that the value of the S decrease with increasing temperature [20]. Also the index S can be determined from the slope of the lnσ-lnω curve [21]. The values of S have been collected in table. 2. It can be seen the agreement of the decrease of S with temperature with the CBH model described by equation.4.

[Downloaded from ndea10.khu.ac.ir on 2026-11-02]

Table2. Dependence of the index S on temperature and frequency

Frequency range	300K	316K	355K	378K
100-1000 Hz	0.0865	0.0842	0.0708	0.0595
1000-10000Hz	0.152	0.136	0.107	0.0899
10000-100000Hz	0.253	0.230	0.217	0.213

Conclusion

PSi layers with different anodization parameters such as current density and anodization time interval were prepared and TiO_2 thin films were deposited with an EBPVD method on the surface of PSi layers. We investigated the morphology of all PSi layers and TiO_2 thin film by electron microscopy. The SEM image shows the porosity of layers increase with increasing current density and anodization time. The effects of current density and anodization time interval on electrical properties were investigated by performing I-V measurement. All samples showed rectifying junction response with applied voltage. We also studied the temperature dependence of the AC electrical conductivity in the Al/TiO_2/PSi/Al nanostructures. The results show that over the range of frequency < 10^3 Hz the band theory and over the range of frequency>10^3 Hz the hopping mechanism with power is applicable to explain the conduction process in Al/TiO_2/PSi/Al nanostructures.

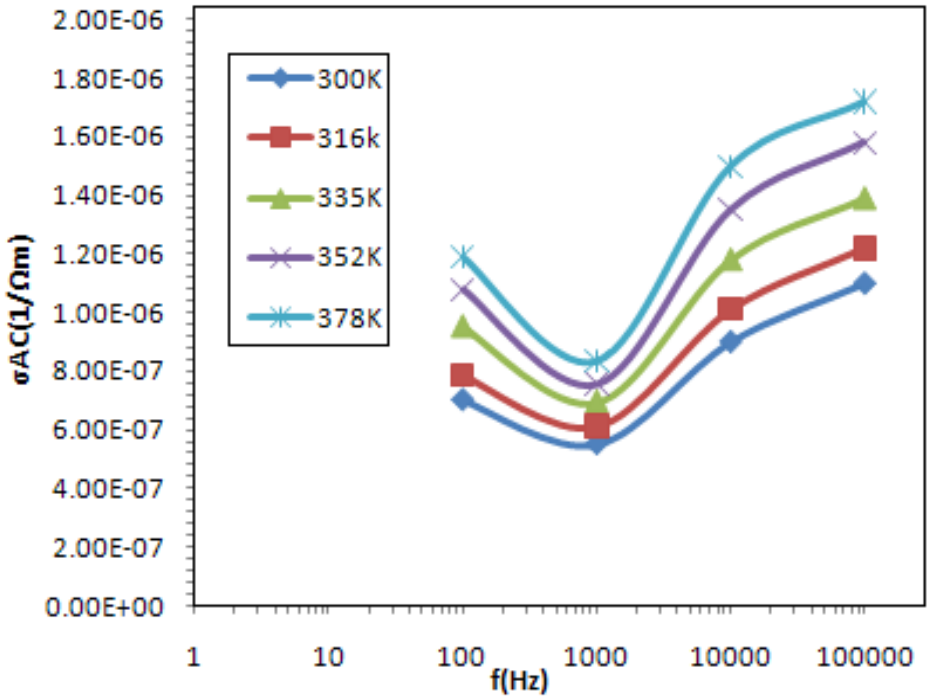


Fig. 5. Dependence of AC conductivity on frequency at different constant temperatures

[Downloaded from ndea10.khu.ac.ir on 2026-11-02]

References

1. V. M. Makara, M. M. Melnichenko, K. V. Svezhentsova, L. Yu. Khomenkova, O. M. Shmyryeva, Semicond, Phys. Quantum Electron, Optoelectron 6 (2003) 492-495.
2. M. A. Vasquez-A, G. Aguila Rodriguez, G. Garcia-Salgado, G. Romero-Paredes, R. Pena-Sierra, Rev. Mex .Fis, 53 (2007) 431-435.
3. S. Ozdmir, J. L. Gole, Curr, Opin, Solid, St. M. 11 (2007) 92-100.
4. M. Thust,M. J. Schoning, S. Frohnhoff, R. Arens-Fischer, P.Kordos, H. Loth, Meas, Sci, Technol 26 (1996) 7.
5. G. O'Halloran, M. Kuhi, P. Sarro, P. Gennissen, P. French, Meetings Abstracts, Spring Meeting of the Electrochemical Society 96 (1996) 414.
6. Y. Zhao, Z. Lv, L. Wang, J. Min, W. Shia, X. Lu, Curr. App. Phys 10 (2010) 930-933.
7. V. Aroutiounian, V. Arkelyan, V. Galstyan, Ieee sensors Journal 9 (2009) 9-12.
8. M. M. Hasan, A. S. M. A. Haseeb, R. Saidur, H. H. Masjuki, Int. J. Chem. Biol. Eng 1:2 (2008) 92-98.
9. Y. M. Sung, H.J. Kim, Thin Solid Films 515 (2007) 4996-4999.
10. W. Yang, C.A. Wolden, Thin Solid Films 515 (2006) 1708-1713.
11. C. Euvananont, C. Junin, K. Inpor, P. Limthongkul, C. Thanachayanont, Ceram, Int 34 (2008) 1067-1071.
12. C. J. Tavares, J. Vieira, L. Rebouta, G. Hungerford, P. Coutinho, V. Teixeira, J.O. Carneiro, A. J. Fernandes, Mat. Sci. Eng: B 138 (2007) 139-143.
13. K. J. Kim, G.S. Kim, J.S. Hong, T.S. Kang, D. Kim, Sol, Energy 64 (1998) 61-66.
14. Sh. D. Milani, R. S. Dariani, A. Mortezaali, V. Dadmehr, K. Robbie, J. Optoelectronics, Adv. Mater 8 (2006) 1216-1220.
15. M. Hwan an, J. Korean. Phys. Soc 47 (2005) 847-851.
16. A. Langer, M. Knez, F. Muller, U. Gosele, appl. Phys. A 93 (2008) 399-403.
17. P. Menna, G. Di Francia, V-La. Ferrara, Sol, Energy, Mater, Sol, cells 37 (1995) 13.
18. M. E. Azimaraghi, Ind. J. Pure Appl. Phys 45 (2007) 40-43.

[Downloaded from ndea10.khu.ac.ir on 2026-11-02]

19. F. Yakuphanoglu, Y. Aydogdu, U. Schatzschneider, E. Rentschler, "Solid State", Commun 128/2-3 (2003) 63-67

20. M. E. Azimaraghi, S. Abasi, J. Optoelectronics, Adv. Mater 12 (2010) 1777-1780

21. R. D. Gould, S. A. Awan, "Thin Solid Films", 433 (2003) 309-314

[Downloaded from ndea10.khu.ac.ir on 2026-11-02]